Current Injection Transition Broadening in Quantum Cascade Lasers

Scott S. Howard, Anthony J. Hoffman, Kale J. Franz, Tiffany Ko, Deborah L. Sivco, and Claire F. Gmachl

***Abstract*—We show control over the linewidth of the fundamental transition in Quantum Cascade lasers by varying the injection barrier thickness and doping in the injector. Additionally, electroluminescence studies allow us to find the states electrons are being injected into as well as the effect of indirect and direct injection into the upper laser level on the transition linewidth broadening.**

Index Terms— **Optical gain, midinfrared, quantum cascade (QC) laser.**

I. Introduction

HIGH performance Quantum Cascade (QC) lasers have demonstrated excellent device characteristics for above-room temperature continuous wave operation [1-2]. Advanced conduction band energy designs have allowed for reduced threshold current density, which improves temperature performance, conversion efficiency, and maximum output power [3]. Advanced models for the self-consistent solutions to both the temperature dependent threshold current density equation and heat equation provide the ability to design laser waveguides specifically for high-temperature operation. A thorough understanding of the linewidth of the transition from the upper to the lower laser level as a function of design parameters, temperature, current, and applied electric field will allow us to further improve our ability to design QC lasers by improving our design parameters as well as give insight to the operation of a typical laser design at optimal and high electrical fields.

II. Experiment

A series of four samples was grown by molecular beam epitaxy (MBE) consecutively with similar conduction band structure to [4], as shown in Fig. 1, by varying injector doping levels and the thickness of the injector barrier as described in Table I. To reduce growth time and drift between samples, the devices consisted 20 periods of active regions and injectors only capped by 0.5 µm of GaInAs lattice matched to InP. The devices were fabricated into circular mesas, ~200 µm in diameter, with a top gold electrical contact and the bottom electrical contact made through the substrate. The samples were cleaved so that 75% of the circular mesa remained with the cleaved facet as the edge emitter.

S. S. Howard, A. J. Hoffman, K. Franz, T. Ko, and C. Gmachl are with Princeton University, Princeton, NJ 08544 USA (e-mail: showard@princeton.edu).

D. L. Sivco is with Alcatel-Lucent Technologies, Murray Hill, NJ 07974 USA.

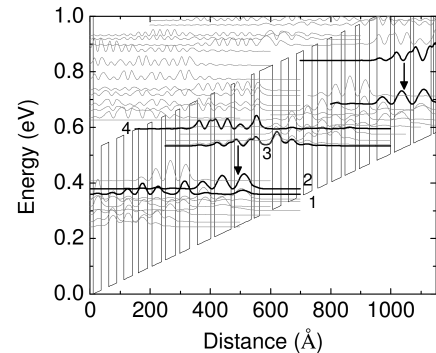

Fig.1. Conduction band energy diagram and moduli squared of wavefunctions for devices D3292 and D3294 at the design field of ~50 kV/cm. D3295 and D3296 are similar with a larger injection barrier. Relevant states are labeled, and the optical transition is indicated by the downward pointing arrow.

TABLE I

	$t_{\text{inject. barrier}}$ = 40 Å	$t_{\text{inject. barrier}}$ = 60 Å
$n_{2D} = 1\text{x}10^{11}$ cm^{-2}	D3292●	D3295■
$n_{2D} = 2\text{x}10^{11}$ cm^{-2}	D3294◇	D3296★

III. Results

Temperature dependent current-voltage curves were measured for the samples in pulsed operation of 100 ns pulses at 3 kHz as seen in Fig. 2. The low doped samples exhibit Stark-effect features and have a larger field dropped across the active region and injectors, and thus allowing for possible injection into high energy levels in the active region. The samples with thin injection barriers show less of a dependence on doping, but still exhibit a high differential resistance region and indirect injection when low doped low. The increased differential resistance seen at ~6-7 V could then be controlled (and minimized) by a combination of injection barrier thickness and doping level of the injector.

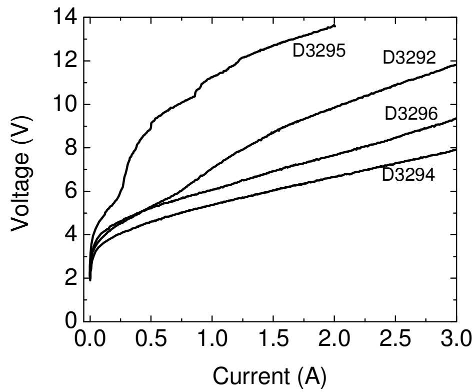

Fig. 2. Current-voltage characteristics of the four samples at 80 K in pulsed mode.

Electroluminescence was measured using a Nicolet Magna-IR 860 FTIR and cooled MCT detector in step scan mode while operating the device with 700ns pulses at 80 kHz repetition rate. Three peaks corresponding to the upper to lower laser level ($3\rightarrow 2$), upper laser level to first extractor level ($3\rightarrow 1$), and active region level above the upper laser level to the lower laser level ($4\rightarrow 2$) were visible as evident in Fig. 3a and 3b. Additionally, the half-width at half-maximum intensity of the transitions is plotted as an upwards error bar for low doped samples and downwards error bar for high doped samples. From these results, it is evident that the transition energies do not change, even at fields > 2 times the design electric field. Additionally, it shows that carriers are being injected into the states above the upper laser level, which causes indirect scattering from the injector into the upper laser level.

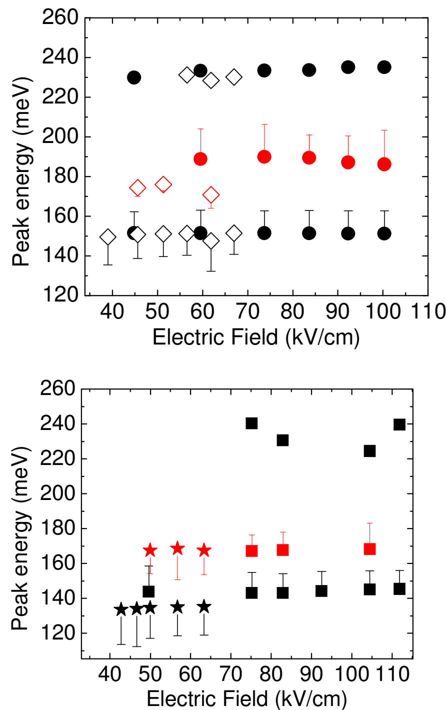

Fig. 3. Transition energy for samples a) D3292 and D3294 (top) and b) D3295 and D3296 (bottom) at 80 K in pulsed mode. Error bars indicate half-width at half-maximum intensity.

Plotting the full-width at half-maximum (FWHM) intensity as a function of the applied field for the various samples in Fig. 4 shows that the linewidth decreases rapidly as it approaches the design field for high-doped samples, while low-doped samples are always at smaller linewidths. Additionally, as the field increases above the design electric field, and indirect injection into the upper laser level increases, the transition linewidth remains small for the low doped samples.

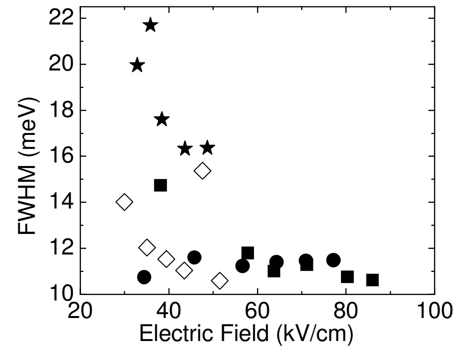

Fig. 4. FWHM as a function of applied electrical field at 80 K in pulsed mode.

By examining the minimum FWHM of the transition at 80 K and 150 K in Fig. 5, one can see the general trend of increasing broadening with increased temperature. Additionally, the large discrepancy in linewidth between the low and high doped thick injection barrier sample, as compared to the thin injection barrier sample, shows that the former is more sensitive to doping.

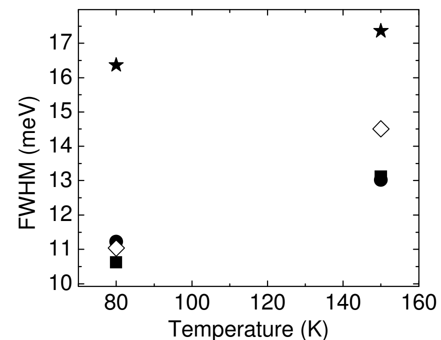

Fig. 5. Minimum FWHM of fundamental transition as a function of temperature in pulsed mode.

ACKNOWLEDGMENT

This work was in part supported by DARPA-EMIL.

REFERENCES

[1] M. Beck, et al., "Continuous wave operation of a mid-infrared semiconductor laser at room temperature," *Science* 295, 301-305 (2002).

[2] L. Diehl, et al., "High-power quantum cascade lasers grown by low-pressure metal organic vapor-phase epitaxy operating in continuous wave above 400 K," *Appl. Phys. Lett*., vol. 88, 201115, 2006.

[3] J. Faist, et al. "Bound-to-continuum and two-phonon resonance quantum-cascade lasers for high duty cycle, high-temperature operation," *IEEE J. Quantum Electron*., 38 (6): 533-546, 2002.

[4] Z. Liu, et al., "Room-temperature CW QC lasers grown by MOCVD without lateral regrowth," IEEE *Photon. Technol. Lett.* 18, 1347-1349, 2006.